Theoretical Studies of the Decomposition of RDX in Liquid Xenon

Yin Guo and Donald L. Thompson*

Department of Chemistry, Oklahoma State University, Stillwater, Oklahoma 74078-0444

Received: June 23, 1999; In Final Form: September 16, 1999

The unimolecular dissociation of RDX (hexahydro-1,3,5-trinitro-1,3,5-triazine) in liquid xenon is investigated to determine condensed-phase effects on the N−N bond fission and ring-opening reactions. The dependence of the rate constants on pressure at a fixed temperature is studied using molecular dynamics simulations, and the result is consistent with the experimental finding that the ring-opening channel is suppressed in a condensed-phase environment. The effects of intramolecular vibrational energy redistribution (IVR) and intermolecular energy transfer on reaction rates are also studied by putting a "hot" RDX molecule in liquid xenon. The reaction rates are calculated using a statistical approach and direct simulations. The statistical rate for the bond fission is 45% larger than the corresponding dynamical one, indicating that the rate of IVR is not faster than that of reaction.

I. Introduction

The unimolecular dissociation reactions of RDX have been the subject of many experimental[1−8] and theoretical studies.[9−13] The experiment of Zhao et al.[1] suggested two competitive primary reaction channels for the thermal decomposition of gas-phase RDX (see Figure 1): the simple N−N bond rupture giving the radicals NO_2 and $C_3H_6N_5O_4$, and the concerted ring-opening reaction that yields three $CH_2N_2O_2$ molecules. The experimentally determined branching ratio of the two channels is about 2. However, the ring fission reaction has not been observed in liquid and solid RDX.

We have carried out a series of classical trajectory and Monte Carlo variational transition-state theory (MCVTST) studies[9−15] on RDX in an effort to develop a potential-energy surface (PES) for it, and to understand the fundamental reaction mechanism, conformational changes in the gas and condensed phases, and unimolecular dissociation processes. In the gas-phase experiment of Zhao et al.,[1] the energy range of the molecule is estimated to be 150−170 kcal/mol, which is too low to perform trajectory simulations because of the long integration time required. However, good agreement with the experiment on the branching ratio has been obtained from MCVTST calculations (see Figure 6 of ref 12) using the PES developed by Chambers and Thompson,[11] suggesting that the PES has the correct features in describing the bond and ring fission reactions in the gas phase.

In the present work, we extend our previous studies of the unimolecular dissociation of RDX in gas phase to condensed phases. The focus is on the condensed-phase effects on the dissociation rates due to the presence of the environment. Rather than attempt the arduous task of realistic simulations of solid or liquid RDX, we have chosen to use a model system with the RDX molecule embedded in liquid xenon. To assess the condensed-phase effects, we perform molecular dynamics simulations to obtain the reaction rates for the bond and ring fissions and compare them to the gas-phase results. Since good agreement with experiment has been obtained for the gas-phase branching ratio using the PES developed by Chambers and Thompson,[11] we use the same PES for RDX in this study.

To investigate the experimental findings that the ring fission is competitive with the bond rupture in the gas phase but not observed in condensed phases, we set the RDX molecule to be in thermal equilibrium with liquid Xe and follow the trajectories to obtain the rate constants. Calculations are performed at different liquid densities to study the dependence of the rates on the pressure.

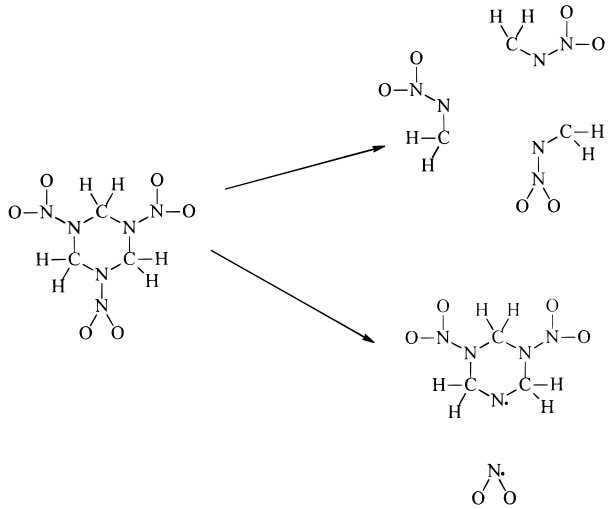

Figure 1. Schematic illustration of RDX.

Another interesting issue is the characteristics of intra- and intermolecular energy transfer and their effects on the reaction rates. To gain some insight into this, we put a vibrationally hot RDX molecule in a cooler liquid and monitor the energy loss from the molecule to the solvent. If the rate of intramolecular vibrational energy redistribution (IVR) is much faster than that of the intermolecular energy flow, the reaction can be treated by a statistical approach. Such an approach only requires the calculation of the energy decay rate of the molecule, which usually takes less computational time, especially at low energies, than does directly following the trajectories to dissociation. We thus compute the rates using both statistical treatment and direct dynamics simulations to explore the applicability of the statistical approach and also to get a better understanding of the intra- and intermolecular energy flow in this kind of complex systems.

10.1021/jp992096t CCC: $18.00
Published on Web 11/13/1999

TABLE 1: Lennard-Jones Potential Parameters

atom pair	ϵ (kcal/mol)	σ (Å)
Xe−Xe	0.461	3.98
Xe−H	0.089	3.40
Xe−C	0.217	3.67
Xe−N	0.185	3.65
Xe−O	0.238	3.47

II. Potential Energy and Simulation Procedures

The total potential is the sum of three terms: the RDX intramolecular potential (taken from ref 11), the RDX−Xe atom−atom interactions, and the Xe−Xe atom−atom interaction. The RDX intramolecular potential includes two reaction pathways, the N−N bond fission and the concerted ring opening. The N−N bond is modeled by a Morse oscillator with a dissociation energy of 47.8 kcal/mol. A plot of potential energy along the minimum-energy path for the ring fission is given in Figure 2 of ref 11 with a barrier height 37 kcal/mol. The intermolecular RDX−Xe and Xe−Xe interactions are assumed to be a sum of pairwise Lennard-Jones 12-6 potentials

$$V_{i,j} = 4\epsilon\left[\left(\frac{\sigma}{r_{i,j}}\right)^{12} - \left(\frac{\sigma}{r_{i,j}}\right)^{6}\right] \quad (1)$$

The parameter values for σ and ϵ for the same atoms were taken from refs 16 and 17, and the values for the interaction between A and B atoms were obtained using the standard combination rules[16]

$$\sigma_{A-B} = \frac{1}{2}(\sigma_A + \sigma_B) \quad (2)$$

$$\epsilon_{A-B} = (\epsilon_A \epsilon_B)^{1/2} \quad (3)$$

The Lennard-Jones potential parameters used in this study are listed in Table 1.

The system consists of 256 xenon atoms plus a RDX molecule initially placed at the center of the simulation box. The initial conditions for the RDX molecule were generated by using the efficient microcanonical Monte Carlo sampling technique developed by Nordholm and co-workers.[18] With the RDX molecule held fixed, the liquid xenon was prepared using a standard warm-up procedure by first assigning momentum randomly to each Xe atom according to a Boltzmann distribution and then running the trajectories and periodically scaling the momenta of all the Xe atoms to the desired temperature. After the initial warm-up period, both the RDX molecule and the xenon atoms were propagated and the desired physical properties were monitored. Periodic boundary conditions were imposed throughout. The highest liquid density used in this work is 0.6 atoms/Å^3. The corresponding box length L with 256 xenon atoms is 30 Å, and half of L is more than the common choice for the cutoff distance 2.7σ (10.7 Å). Thus, the use of 256 xenon atoms should be sufficient for describing the interactions between the RDX molecule and the liquid and also to permit the neglect of the interactions from the images of the molecule itself. A Runge−Kutta−Gill integrator was used with step sizes of 0.1 fs for the RDX molecule and 0.5 fs for the xenon atoms.

III. Results and Discussion

The primary decomposition channels of gas-phase RDX are assumed to be the simple N−N bond rupture and the concerted ring fission (see Figure 1). In the gas-phase calculations, we assumed the N−N bond breaking reaction to have occurred when the N−N bond length exceeded 5.5 Å, and a ring-opening reaction to have occurred when the C−N bond length exceeded 5.8 Å. The simulations show that a critical bond length of around 3 Å is sufficient for both channels. In the condensed-phase calculations, we took the critical bond length to be 11 Å for both the N−N and C−N bonds to ensure that the fragments are truly separated.

TABLE 2: Microcanonical Rate Constants for the N−N Bond Rupture and Ring Fission Channels of the Decomposition of RDX

energy (kcal/mol)	k^0_{bond} (ps^{-1})	k^0_{ring} (ps^{-1})
200	0.0038	0.0025
225	0.015	0.0067
250	0.045	0.019
300	0.21	0.067
325	0.37	0.11
350	0.60	0.15
400	1.4	0.37
450	2.2	0.53

To investigate the experimental findings that the ring fission channel is competitive in the gas phase but not present in condensed phases, we model the effects of the environmental confinement by letting the RDX molecule to be initially in thermal equilibrium with the xenon atoms. This allows us to study the effect on the reaction rates due to the structural presence of the solvent, not the net energy flow between the molecule and the bath. The calculated rates are then compared to the gas-phase results.

Also of interest are the roles of intramolecular vibrational energy redistribution and intermolecular energy transfer in the reaction dynamics. To study these effects on the reaction rates, we put a "hot" RDX molecule in liquid xenon and monitor the energy flow from the molecule to the bath. After obtaining the energy decay rate, we use a statistical treatment to calculate the reaction rates and compare them with those obtained from direct dynamics simulations. Our goal is to gain some insight into the relative importance of intra- and intermolecular energy transfer and to explore the possibility of using a statistical approach to the problem.

The gas-phase results have been previously given by Chambers and Thompson.[11] To reduce the statistical errors, we have recalculated rates on the same potential-energy surface by using larger ensembles of 1000−2000 trajectories. The rate constants for the two channels are given in Table 2. The data were also fitted to the RRK expression

$$k(E) = \nu\left(1 - \frac{E_b}{E}\right)^s \quad (4)$$

as shown in Figure 2, with $E_b = 47.8$ kcal/mol, $\nu = 0.21$ fs^{-1}, $s = 40$ for the bond fission, and $E_b = 37$ kcal/mol, $\nu = 0.028$ fs^{-1}, $s = 46$ for the ring fission.

A. RDX Molecule in Thermal Equilibrium with Liquid Xenon. The RDX molecule was set to be initially in thermal equilibrium with liquid Xe by assigning the total energy of the molecule $E = 3Nk_BT$ ($N = 21$); i.e., the average energy per degree of freedom is equal to the thermal energy. In the study presented in this subsection, the initial total energy of the RDX molecule was chosen to be 250 kcal/mol, and accordingly, the solvent temperature was set at 2000 K. Note that in relating the molecular energy with the temperature we have assumed all the degrees of freedom are classical and also employed the harmonic approximation. Since the energy per mode is (250/63) kcal/mol = 3.97 kcal/mol, this harmonic approximation should not lead to significant errors. Calculations were per-

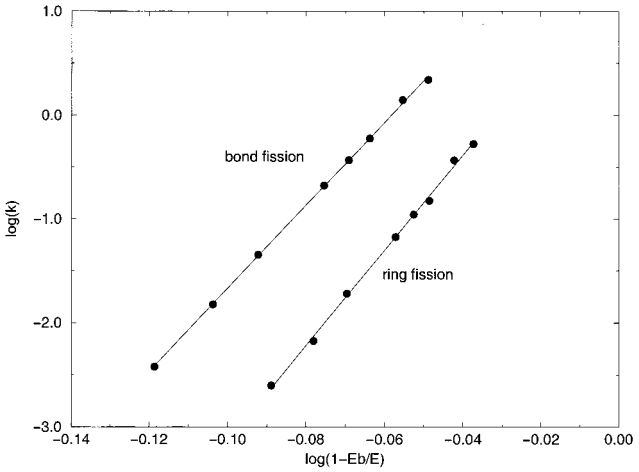

Figure 2. Calculated microcanonical rates for the two reaction channels of RDX. The lines are the RRK fits.

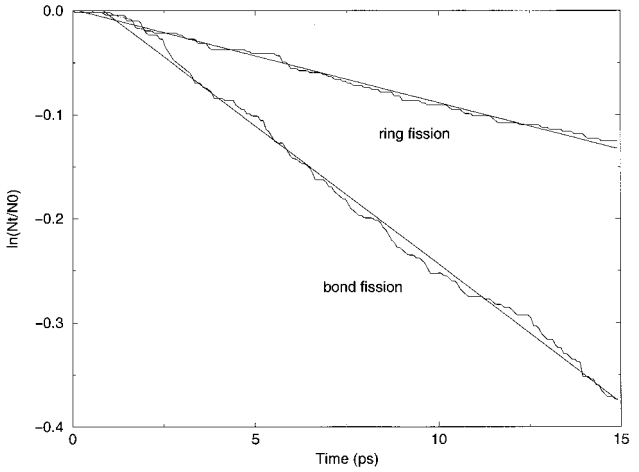

Figure 3. Typical decay curves for the two reaction channels of RDX in liquid Xe from trajectory simulations. Here the density of the liquid is 0.5 atoms/Å^3.

TABLE 3: Rate Constants for the N−N Bond Rupture and Ring-Opening Channels of the Decomposition of RDX in Liquid Xenon[a]

density (atoms/Å^3)	k_{bond} (ps^{-1})	k_{ring} (ps^{-1})
0.0	0.045	0.019
0.1	0.040	0.017
0.3	0.036	0.014
0.5	0.027	0.0090
0.6	0.021	0.0059

[a] The temperature is 2000 K, and the initial energy of RDX is 250 kcal/mol. The first row is the gas-phase result.

formed for four different liquid densities 0.1, 0.3, 0.5, and 0.6 atoms/Å^3. Ensembles of 450−650 trajectories were used.

The reaction rate for each of the two channels was assumed to be first order, so the rate constant k was obtained by fitting the decay curve to

$$\ln(N_t/N_0) = -kt \tag{5}$$

where N_t is the number of unreacted trajectories at time t and N_0 is the total number of trajectories in the ensemble. Figure 3 shows typical decay plots (for density of 0.5 atoms/Å^3). The lines are the least-squares fits. The calculated rate constants for both channels at four solvent densities are given in Table 3.

Figure 4 illustrates the dependence of the rate constants on pressure, ln k versus P. The pressure was obtained from the

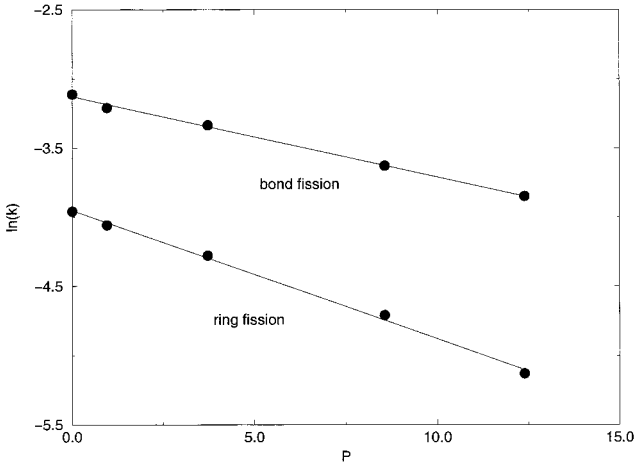

Figure 4. Dependence of the rate constants on pressure. The units of the pressure are 5.0 × 10^2 atm.

density by using an equation of state for the Lennard-Jones fluid[19]

$$P/T^*\rho^* = 1 + B_1x + B_2x^2 + B_3x^3 + B_4x^4 + B_{10}x^{10} - (T^*)^{-1}\sum_{i=1}^{5} iC_ix^i \tag{6}$$

where $T^* = k_BT/\epsilon$, $\rho^* = \rho\sigma^3$, and $x = \rho^*(T^*)^{-1/4}$. The coefficients are $B_1 = 3.629$, $B_2 = 7.2641$, $B_3 = 10.4924$, $B_4 = 11.459$, $B_{10} = 2.17619$, and $C_1 = 5.3692$, $C_2 = 6.5797$, $C_3 = 6.1745$, $C_4 = -4.2685$, $C_5 = 1.6841$. The result of Figure 4 is in accord with the usual expression for the reaction rates under hydrostatic pressure first formulated by van't Hoff

$$\ln k = \ln k^0 - \Delta V^{\ddagger}P/RT \tag{7}$$

where $\Delta V^{\ddagger}$ is the volume of activation. The values calculated for $\Delta V^{\ddagger}$ from the slopes of the least-square fitted lines shown in Figure 4 are 30 cm^3/mol for the ring fission and 19 cm^3/mol for the bond rupture. Thus, the rate of the ring fission decreases faster with increasing pressure than that of the bond rupture. The ratio of the two rates, k_{ring} and k_{bond}, as a function of pressure can be obtained from eq 7

$$\ln (k_{ring}/k_{bond}) = \ln(k^0_{ring}/k^0_{bond}) - (\Delta V^{\ddagger}_{ring} - \Delta V^{\ddagger}_{bond})P/RT \tag{8}$$

The results here suggest that the ring fission is reduced more in the presence of an environment, thus providing a plausible explanation to the experimental fact that it was not observed in condensed phases.

B. "Hot" RDX Molecule in Liquid Xenon. The RDX molecule was assigned an initial total energy E_0 such that the average energy per mode is larger than the thermal energy, $E/3N > k_BT$, that is, the molecule is hotter than the liquid. There are two factors due to the presence of the liquid that reduce the unimolecular reaction rate: (1) the net energy loss of the molecule to the bath, and (2) the effects due to the spatial confinement of the bath. To a first approximation, we assume these two factors can be treated separately. Then the ratio of the decrease in the total rate, i.e., the ratio of the total rate constant k in the presence of the liquid to the gas-phase rate k^0, can be written as a product of the ratios of the decreases in the rates due to the aforementioned factors (1), k_1/k^0, and (2), k_2/k^0:

$$\frac{k}{k^0} = \frac{k_1}{k^0}\frac{k_2}{k^0} \tag{9}$$

where k_1 and k_2 are the rate constants due to factors (1) and (2), respectively. The calculation of k_2 has been given in the preceding subsection.

We can assume k_1 is the result of a statistical process. Thus, we assume k_1 depends only on the total energy of the RDX molecule. Since the energy of the molecule varies with time as it flows to the bath, the rate constant should also be time dependent. Assuming the system is statistical, the rate constant can be expressed as

$$k(t) = \int f(E,t)\, k(E)\, \mathrm{d}E \tag{10}$$

where $k(E)$ is the microcanonical rate and $f(E,t)$ is the energy distribution of the molecule at time t. To simplify the calculation, we approximate $f(E,t)$ as a δ-function concentrated at the average energy of the molecule $\langle E(t)\rangle$, that is

$$f(E,t) = \delta(E - \langle E(t)\rangle) \tag{11}$$

From the energy diffusion theory,[20] $\langle E(t)\rangle$ is of the form

$$\langle E(t)\rangle = k_\mathrm{B}T + (E(0) - k_\mathrm{B}T)\mathrm{e}^{-at} \tag{12}$$

if the energy flow is diffusive. In our case, the thermal energy $k_\mathrm{B}T$ is much smaller than the energy of the molecule and thus can be neglected. Equation 12 then becomes

$$\langle E(t)\rangle = E(0)\mathrm{e}^{-at} \tag{13}$$

Combining eqs 4, 11, and 13, eq 10 becomes

$$k(t) = \nu\left(1 - \frac{E_\mathrm{b}}{E(0)\mathrm{e}^{-at}}\right)^s \tag{14}$$

The time dependence of the decay is then of the following nonlinear form

$$\ln(N_\mathrm{t}/N_0) = -\int_0^t k(\tau)\,\mathrm{d}\tau = -\int_0^t \nu\left(1 - \frac{E_\mathrm{b}}{E(0)\mathrm{e}^{-a\tau}}\right)^s \mathrm{d}\tau \tag{15}$$

which gives the time-dependent rate k_1. Thus, the essence of this statistical treatment is to first compute the energy decay rate a by molecular dynamics and then use it in eq 15 to obtain the decay rate. The advantage of such an approach is that it usually only requires relatively short-time dynamics to obtain the energy decay rate a, thus providing a time saving method for treating large systems.

Since the energy decay rate a is fairly small in the case studied here, the decay curve given by eq 15 is approximately linear. We thus calculate the statistical rate constant k_1 by fitting the decay curve of eq 15 to

$$\ln(N_\mathrm{t}/N_0) = -k_1 t \tag{16}$$

and then compare the total statistical rate k_1k_2/k^0 to the simulation result obtained using the same type of linear fitting.

The RDX molecule was initially assigned a total energy of 350 kcal/mol, so the average energy per mode is 5.56 kcal/mol, which is more than the thermal energy of 3.97 kcal/mol (2000 K) of the liquid Xe. The density of the liquid was chosen to be 0.3 atoms/Å^3. An ensemble of 700 trajectories was used.

Figure 5 shows the ensemble-averaged energy of the RDX molecule as a function of time. Fitting the curve to the exponential form of eq 13 yields the energy decay rate a = 0.0145 ps^{-1}. The rate constant k_1 can then be obtained by plotting the decay curve of eq 15 and fitting it to eq 16, as shown in Figure 6. The calculated statistical rate k_1 is 0.519 and 0.146 ps^{-1} for the bond and ring fissions, respectively. The total rate can then be computed using eq 9, yielding $k = k_1k_2$-$(E(0) = 250)/k^0$ ($E = 250$) = 0.42 and 0.11 ps^{-1} for, respectively, the bond and ring fission channels. The direct dynamics simulation results obtained from fitting the decay curves given in Figure 7 are $k_\mathrm{bond} = 0.29$ ps^{-1} and $k_\mathrm{ring} = 0.11$ ps^{-1}. The statistical treatment gives an accurate rate for the ring fission but a 45% overestimate for the bond rupture. A plausible explanation is that the IVR is not fast enough for the energy lost from the molecule to the bath to be statistically distributed among the modes as the RRK formula assumes. The energy loss in the breaking bond may be more than the statistical average energy loss in the other modes, leading to a lower rate than that predicted by the statistical approach.

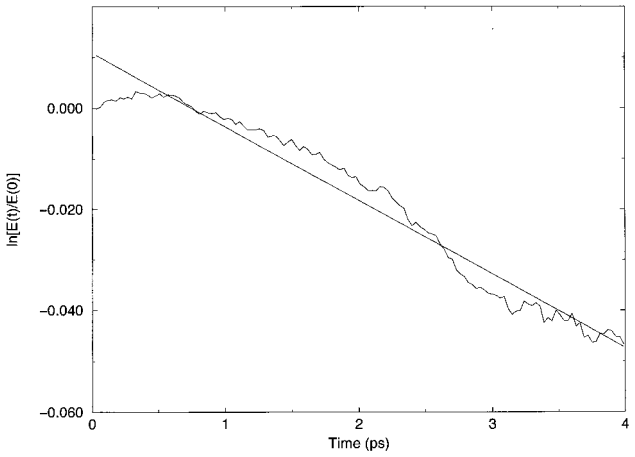

Figure 5. Plot of the ensemble-averaged energy of the RDX molecule as a function of time. The line is the least-squares fit of the curve which gives the energy decay rate.

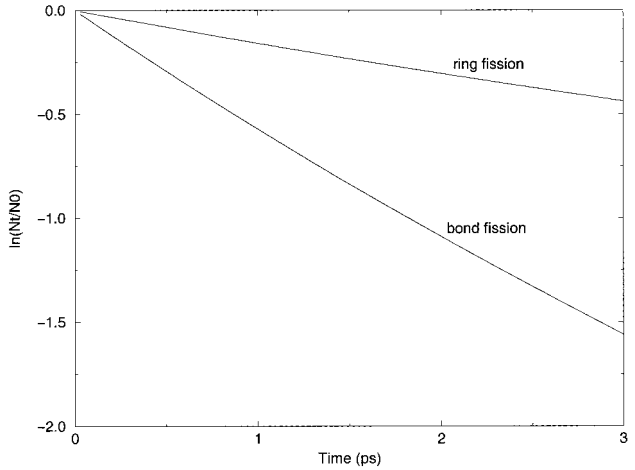

Figure 6. Plots of decay curves using eq 15 for the bond and ring fissions in RDX.

IV. Summary

We have investigated the condensed-phase effects on the unimolecular dissociation of RDX by using a model system consisting of a RDX molecule and liquid Xe. To investigate why the ring fission is competitive with the simple N−N bond rupture in the gas phase but apparently not in the liquid and solid phases, molecular dynamics simulations were carried out

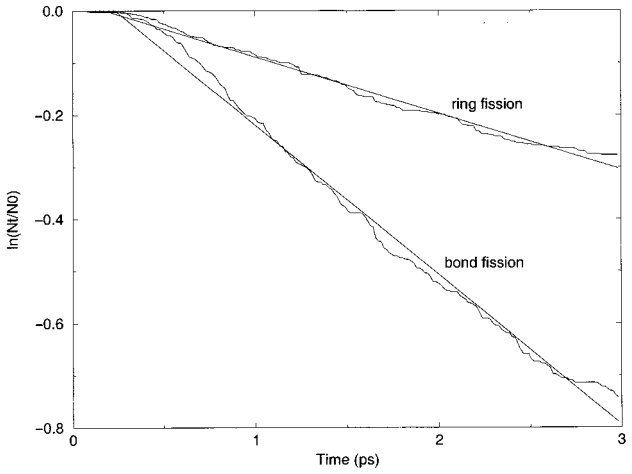

Figure 7. Plots of decay curves from trajectory simulations for the bond and ring fissions in RDX. The RDX molecule is initially "hotter" than the liquid.

to obtain the rates for the two channels by assigning the RDX molecule an initial energy in such a way that the average energy per mode is equal to the thermal energy. The calculated volume of activation is 30 cm^3/mol for the ring fission and 19 cm^3/mol for the bond rupture, suggesting that the ring fission reaction is suppressed more in the confines of an environment and thus providing a plausible explanation to the experiments.[21] We have also investigated the effects of inter- and intramolecular energy transfer on the reactions by assigning RDX an initial energy such that the average energy per mode is higher than the thermal energy. The reaction rates were computed using a statistical method and direct dynamics simulations. The statistical method requires only the calculation of the energy decay rate of the molecule, which is often computationally less expensive than following the trajectories to dissociation. The calculated statistical rate for the ring fission agrees well with the dynamical rate, whereas it is 45% larger than the dynamical rate for the bond fission, indicating that the IVR there is not faster than reaction.

Acknowledgment. This work was supported by the U.S. Army Research Office, Grant No. DAAG55-98-l-0089.

References and Notes

(1) Zhao, X.; Hintsa, E. J.; Lee, Y. T. *J. Chem. Phys.* **1988**, *88*, 801.
(2) Oyumi, Y; Brill, T. J. *J. Phys. Chem.* **1987**, *91*, 3657.
(3) Brill, T. B.; Brush, P. J.; James, K. J.; Shepherd, J. E.; Pfeiffer, K. J. *J. Appl. Spectrosc.* **1992**, *46*, 900.
(4) Behrens, Jr., R.; Bulusu, S. *J. Phys. Chem.* **1991**, *95*, 5838.
(5) Behrens, Jr., R.; Bulusu, S. *J. Phys. Chem.* **1992**, *96*, 8877.
(6) Behrens, Jr., R.; Bulusu, S. *J. Phys. Chem.* **1992**, *96*, 8891.
(7) Botcher, T. R.; Wight, C. A. *J. Phys. Chem.* **1993**, *97*, 9149.
(8) Adams, G. F.; Shaw, Jr., R. W. *Annu. Rev. Phys. Chem.* **1992**, *43*, 311.
(9) Sewell, T. D.; Thompson, D. L. *J. Phys. Chem.* **1991**, *95*, 6228.
(10) Sewell, T. D.; Chambers, C. C.; Thompson, D. L.; Levine, R. D. *Chem. Phys. Lett.* **1993**, *208*, 125.
(11) Chambers, C. C.; Thompson, D. L. *J. Phys. Chem.* **1995**, *99*, 15881.
(12) Shalashilin, D. V.; Thompson, D. L. *J. Phys. Chem. A* **1997**, *101*, 961.
(13) Guo, Y.; Shalashilin, D. V.; Krouse, J. A.; Thompson, D. L. *J. Chem. Phys.* **1999**, *110*, 5521.
(14) Wallis, E. P.; Thompson, D. L. *Chem. Phys. Lett.* **1992**, *189*, 363.
(15) Wallis, E. P.; Thompson, D. L. *J. Chem. Phys.* **1993**, *99*, 2661.
(16) Allen, M. P.; Tildesley, D. J. *Computer Simulation of Liquids*; Clarendon Press: Oxford, UK, 1987.
(17) Ashcroft, N. W.; Mermin, N. D. *Solid State Physics*; Saunders College: Philadelphia, PA, 1976.
(18) Schranz, H. W.; Nordholm, S.; Nyman, G. *J. Chem. Phys.* **1991**, *94*, 1487. Nyman, G.; Nordholm, S.; Schranz, H. W. *J. Chem. Phys.* **1990**, *93*, 6767.
(19) Hansen, J. P. *Phys. Rev. A* **1971**, *2*, 221.
(20) Nikitin, E. E. *Theory of Elementary Atomic and Molecular processes in Gases*; Clarendon: Oxford, UK, 1974.
(21) This explanation for the difference in the gas- and condensed-phase mechanisms was originally suggested by Botcher and Wight in ref 7.